Annals of Biomedical Engineering (© 2021)
https://doi.org/10.1007/s10439-021-02731-0

BMES BIOMEDICAL ENGINEERING SOCIETY

Original Article

Assessing Pressure–Volume Relationship in Developing Heart of Zebrafish *In-Vivo*

NABID SALEHIN,[1] CAMERON VILLARREAL,[1] TANVEER TERANIKAR,[1] BENJAMIN DUBANSKY,[2] JUHYUN LEE,[1] and CHENG-JEN CHUONG[1]

[1]Department of Bioengineering, University of Texas at Arlington, Arlington, TX 76010, USA; and [2]Department of Biological Sciences, University of North Texas, Denton, TX 76201, USA

(*Received 23 October 2020; accepted 8 January 2021*)

Associate Editor Stefan M. Duma oversaw the review of this article.

Abstract—During embryogenesis, the developing heart transforms from a linear peristaltic tube into a multi-chambered pulsatile pump with blood flow-regulating valves. In this work, we report how hemodynamic parameters evolve during the heart's development, leading to its rhythmic pumping and blood flow regulation as a functioning organ. We measured the time course of intra-ventricular pressure from zebrafish embryos at 3, 4, and 5 days post fertilization (dpf) using the servo null method. We also measured the ventricular volume and monitored the opening/closing activity of the AV and VB valves using 4D selective plane illumination microscopy (SPIM). Our results revealed significant increases in peak systolic pressure, stroke volume and work, cardiac output, and power generation, and a total peripheral resistance decrease from zebrafish at 4, 5 dpf versus 3 dpf. These data illustrate that the early-stage zebrafish heart's increasing efficiency is synchronous with the expected changes in valve development, chamber morphology and increasing vascular network complexity. Such physiological measurements in tractable laboratory model organisms are critical for understanding how gene variants may affect phenotype. As the zebrafish emerges as a leading biomedical model organism, the ability to effectively measure its physiology is critical to its translational relevance.

Keywords—Developing heart, Cardiac biomechanics, Pressure–volume loops, Zebrafish, Ventricle.

INTRODUCTION

Despite ongoing technological advances, it remains challenging to adequately visualize and study the development of the embryonic human heart. Animal models such as the mouse[17] and bird[3] are widely used to study cardiovascular development and pathogenesis from the level of molecular underpinnings to the associated morphological, behavioral and physiological phenotypes. The zebrafish has emerged as a leading *in vivo* model for developmental biology due to its relatively low cost, fast development in culture, and the fact that its early developmental stages can be imaged using light microscopy due to the relative transparency.[36] Researchers have heavily leveraged the large molecular toolkit available for the fully sequenced and well-annotated zebrafish genome to detect or induce gene-level modifications while monitoring the morphological landmarks of clinically relevant cardiac defects.[16,32] As such, the zebrafish has emerged as a venerable model for studying human cardiovascular developmental defects and diseases.[2,25,39] However, the zebrafish's small size has meant tools to directly measure cardiovascular variables lagging the relatively rapid development of molecular (and behavioral) tools.

In contrast to the four chambered mammalian heart, the zebrafish heart is composed of only two chambers (one ventricle and one atrium).[2] Blood comes from the venous system through the sinoatrial valve into the atrium of the zebrafish heart, which pumps blood through the atrio-ventricular (AV) valve into the ventricle. The ventricle then pumps blood out of the heart through the ventriculo-bulbar (VB) valve into the outflow tract where the bulbus arteriosus (BA) receives the blood under ventricle-generated pressure. This pressure stretches the elastin-rich BA,[22] creating a "capacitor" that stores and releases elastic energy to maintain continuous blood flow away from the heart and into the gills where oxygen and ion transport

Address correspondence to Cheng-Jen Chuong, Department of Bioengineering, University of Texas at Arlington, Arlington, TX 76010, USA. Electronic mail: chuong@uta.edu

Published online: 02 February 2021

occur.[10] The oxygenated blood then flows through the body and back to the heart in a single systemic circuit.[2]

Despite having only two chambers, the zebrafish heart is a venerable model for early cardiovascular development. Early heart development is highly conserved across vertebrates, such that all hearts proceed through the same general developmental landmarks. In zebrafish, the formation of the heart tube starts ~ 16 h post fertilization (hpf) in embryos incubated at 28° C. The tube-shaped heart, which starts to contract in a rhythmic peristaltic manners near 24 hpf, begins to loop into an "S-shape" near 33 hpf in a similar pattern as other vertebrates. Pumping mechanisms transform from slow peristaltic waves into sequential chamber contractions at approximately 36 hpf, just prior to valve formation.[38] As the chambers differentiate, bumps of tissue between the chambers called endocardial cushions start transforming into primitive valve leaflets at ~ 40 hpf. Functional valve development is completed by 96–120 hpf.[26,32] Organogenesis for zebrafish incubated at 28° C is largely completed by 5 days post fertilization[28] (Fig. 1.)

To best leverage the zebrafish developmental program as a model for human cardiovascular pathophysiology, it is crucial to understand the complex physiological phenotypes that may arise from physical and pharmacological stressors as well as from induced and acquired genetic variation.[6] However, it has been difficult to measure relevant cardiovascular parameters such as blood flow, blood pressure and the electrical events that occur during the cardiac cycle in developing zebrafish. Indeed, few devices are available that enable the direct measurement of cardiac physiology in these small model organisms (≈ 4 mm long when newly hatched).

The pressure–volume loop (PV loop) is a tool to visualize changes in pressure and blood volume in the heart ventricles.[13] By incorporating changes in both pressure and volume during the cardiac cycle, the resultant plot of pressure versus volume provides deep physiological insights into ventricular function.[33] Indeed, nuances in PV loops can indicate fine-scale effects from cardioactive stressors such as changes in preload, afterload and inotropy. The embryonic zebrafish's small size, however, has made it challenging to directly measure intra-ventricular pressure and volume. Here, we separately measured ventricular pressure and volume in developing zebrafish *in vivo* at 3, 4 and 5 dpf. We used servo null micro-pressure measurement technology[2,10] to measure intra-ventricular pressure. Next, we used 4-D (3-D + time) selective plane illumination microscopy (SPIM)[15,16] to measure ventricular volume and the function of the AV and VB valves during early development. With this recorded data, we generated PV loops for zebrafish at 3, 4 and 5 dpf and used these measurements to calculate hemodynamic parameters, including stroke volume, heart rate, cardiac output, ejection fraction, stroke work, power, and total peripheral resistance. Collectively, these data describe the improved mechanical performance of the developing zebrafish heart at 3, 4, and 5 dpf. These data provide new insight for assessing hemodynamic parameters in the zebrafish embryo, and strongly highlights the need for reliable technologies to directly measure cardiovascular physiology.

MATERIALS AND METHODS

Zebrafish and Preparation for Imaging

Transgenic zebrafish embryos Tg*(cmlc2:* mCherry*; fli1a:* GFP*)* at 3, 4, 5 dpf expressing mCherry fluorescent signal in myocardium and green fluorescent signal in endocardium were used for imaging and calculating ventricular volume and AV and VB valve analyses in this study. Embryos were bred and maintained at the UT Arlington animal care facility. Embryos were incubated at 28 °C in zebrafish embryo media (E3 media) with 0.003% phenylthiourea (PTU) added at 20 hpf to maintain embryo transparency.[37] For imaging, embryos were anesthetized in 0.05% tricaine and immersed in 0.5% low melting point agarose which was refractive indice-matched to water. Embryos were transferred to a fluorinated ethylene propylene (FEP) tube for embryo mounting and manipulation for light sheet microscopy. Husbandry and experiments were performed in compliance with our Institutional Animal Care and Use Committee (IACUC) protocols.

Image Acquisition

Three separate embryos at each of 3, 4, 5 dpf time point were imaged by SPIM. A laser (CNI Laser, PSU–III-LED) operated at 473 and 532 nm was used to provide the excitation for GFP and mCherry respectively, and a 10X objective lens (NA = 0.2) was used for detection. The illumination and the detection path are orthogonal to each other with the sample placed at the intersection of the two axes. Only the fluorophores in the focal plane of the detection objective lens are excited and the emission light is collected through the detection optics and recorded using a digital camera (Hamamatsu, ORCA Flash 4.0 sCMOS, see schematic in Fig. S1). A single 2D image can thus be obtained at the focal plane without scanning. Dynamic 3D volumes of the embryonic zebrafish heart were acquired by collecting 2D image sequences while moving the sample along the detection axis at a

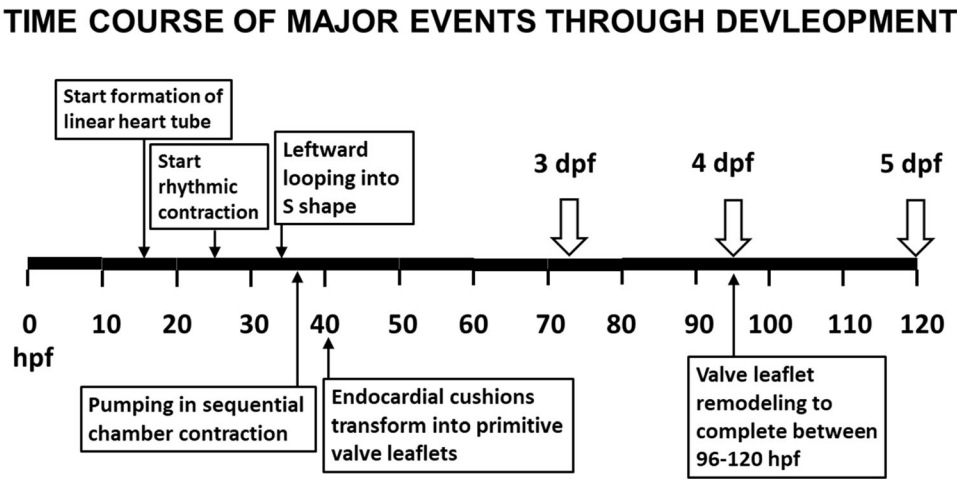

FIGURE 1. Heart development in zebrafish with major milestones indicated.

fixed 2 μm step size. We captured 2D image sequence stacks of the heart from the cranial to the caudal end. Each slice sequence in the stack consisted of 500 frames (512 × 512 pixels), imaged at 10 ms exposure time per frame with 80–120 overlapping z-slices recorded . 4D images were reconstructed from the slice sequences with a voxel size of 0.65 × 0.65 × 2 μm^3. Custom LABVIEW (National Instruments) code was used to control the process of image acquisition and recording.

4-D Images of the Embryonic Zebrafish Heart

Acquired image slices were processed with software we previously developed.[15,16] Briefly, dynamic 3D volumes were reconstructed by a non-gated synchronization algorithm that rearranged the slice sequences to find the minimum error of the cardiac phase of each layer, with respect to time.[19,21] The synchronization algorithm was based on a criterion to minimize least squares intensity differences implemented in custom MATLAB code (MathWorks).

Estimation of Ventricular Volume Reconstructed from 3-D Images

We recovered the dynamic events of the ventricle over cardiac cycles using reconstructed 4D images of the embryonic zebrafish hearts. At each time point through a cardiac cycle, individual slices that made up the ventricular volume were manually segmented to delineate the endocardial surface of the ventricle as well as the positioning of the AV and VB valve leaflets. Figure 2a is a representative slice image from a 5 dpf fish when its AV valve was fully open and VB valve was closed during diastolic filling; whereas Fig. 2b is that when the AV valve was closed and VB valve was fully open during ejection. In both, we added yellow dot lines to delineate the endocardial surface. The corresponding blood volume enclosed by the endocardial surface was calculated as the product of the confined area multiplied by the slice thickness of the image. The instantaneous ventricular blood volume was obtained by summing the volume of the segmented stacks at the time step (Fig. 2c). The stroke volume of the beating heart was then calculated as the difference in the ventricular volume between end-diastole and end-systole states. Image analysis of the volume renderings was performed using Slicer 3D (www.slicer.org).

Calculation of Blood Flow Rate into the Ventricle and Out of the Ventricle to Bulbus Arteriosus (BA)

Knowing the moment-to-moment blood flow rate enables assessment of the effects of the instantaneous driving pressure from the contracting atrium, and the impedance of the ventricle in accommodating the blood influx during filling phase. Likewise, it enables examination of the effect of the instantaneous driving potential of the contracting ventricular myocardium and the impedance of the BA to accommodate the blood influx during ejection phase. In large animals, blood flow rate can be measured by invasive (indicator dilution, radio-labeled tracer washout) or non-invasive (Doppler ultrasound, contrast-enhanced ultrasonography) techniques. Because of the technical difficulty associated with the small size of the embryonic heart, we chose to use an indirect method to calculate the flow rate by taking the time derivative of the reconstructed ventricular volume: $\dot{Q} = \frac{d(\mathrm{vol})}{dt}$. For improved accuracy of the numerical differentiation at each time step, four neighboring time points were considered making up a five-point stencil.

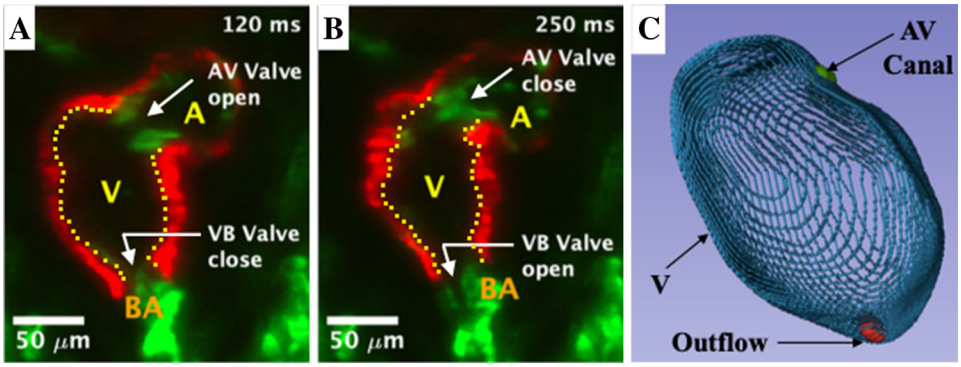

FIGURE 2. SPIM images of the developing Tg(*cmlc2:* mcherry*; fli1a:* gfp) zebrafish heart at 5 dpf, (a) when AV valve fully open and VB valve closed during diastolic filling and (b) when AV valve closed and VB valve fully open during ejection. Yellow dot lines were added for the delineated endocardial surface. Myocardium: Red; Endocardium: Green; Endocardial surfaces: Yellow dot lines; V: Ventricle; A: Atrium; BA: Bulbus arteriosus. (c) Stack of endocardial surface contours based on which we calculated the ventricular volume at each of the time steps in a cardiac cycle. AV canal and outflow are shown in green and red color.

Measurements of Intra-ventricular Pressure and that of BA

Since ventricular pressure measurements are destructive, separate organisms were used for individual ventricular pressure measurements (see Limitations section). Five separate embryos per time point were anesthetized in 0.05% tricaine and placed in an agarose-filled petri dish with customized depressions in the agarose that helped to stabilize the embryo. Intra-ventricular pressure of zebrafish embryos was measured using a 900A servo null micro-pressure system (World Precision Instruments). Briefly, a glass electrode with a 2–5 μm tip diameter was pulled from borosilicate glass and filled with 1 M NaCl and the tip was inserted into the ventricle. Changes in ventricular pressure cause a change in electrical resistance at the tip of the micropipette which is offset by system generated compensatory positive or negative pressure. Known pressure pulses of 5–20 mmHg were used for calibration. Prior to each measurement, the system was recalibrated to zero, such that reported pressures are relative to the external fluid pressure just outside the heart. Data were sampled at 100 Hz and passed through an IIR Butterworth filter to eliminate high frequency noise with cut-off frequency determined from spectrum analysis. Recorded analog signals were filtered using a MATLAB (MathWorks) code. Pressure of the BA from embryos at 3, 4, 5 dpf group were measured by the same steps.

Open–Close Activities of AV and VB Valve

We monitored the time courses AV and VB valve operation during cardiac cycles. The distance between the tips of the two AV valve leaflets was measured in each video image frame to track the valve opening and closure during the cardiac cycle. Embryos at 3 dpf did not yet have working valves and were thus excluded from these analyses. VB valve activity was measured starting at 4 dpf by calculating the change in area of the proximal region of the BA during the cardiac cycle. We considered the VB valve cycle to begin at the instant when the BA area began to increase (due to increasing volume at blood influx), and the VB valve closure process began the moment the BA area started to decrease. Image analysis was performed in MATLAB (MathWorks).

Synchronization of Pressure and Volume

Since pressure and volume cannot yet be measured simultaneously on a single fish, synchronization of data was needed (see Limitations section). We identified the end of isovolumic relaxation and the end of diastole as the respective time points at which the AV valve opened and closed. Similarly, the time points when the VB valve opened, and the VB valve closed respectively marked the start and the end of ejection. From the time course of intra-ventricular pressure, the end of isovolumic relaxation was identified as the time point at which the first derivative of ventricular pressure (dP/dt) reached zero following its minimum. Similarly, the time at which dP/dt started rising sharply toward its maximum value marked the end diastole. For synchronization of pressure and volume, these events in the cardiac cycle were matched in time from the volume-time curve and the pressure-time curve.

Hemodynamic Parameters and the P–V Loops

From the reconstructed ventricular volume time courses, we identified end diastolic volume (EDV), end systolic volume (ESV), stroke volume ($SV = EDV - ESV$), and heart rate (HR) to calculate

cardiac output ($CO = SV \times HR$), and ejection fraction $\left(EF = \frac{(EDV-ESV)}{EDV}\right)$. From intra-ventricular pressure recordings, we identified peak systolic ventricular pressure ($PSVP$) and end diastolic ventricular pressure ($EDVP$). Synchronized pressure and volume were combined to generate the pressure–volume (PV) loops to allow the assessment of cardiac function. We further calculated stroke work from $SW = -\oint p \cdot d(\text{vol})$, the work done by the ventricle in each of the cardiac cycles to enable blood circulation in the cardiovascular system, and the power generation was calculated as ($Power = SW \times HR$). Additionally, we calculated total peripheral resistance (TPR) from $TPR = \frac{\overline{P_{BA}}}{CO} = \frac{1}{CO}\frac{\int_{t_1}^{t_2} P_{BA}(t)dt}{(t_2-t_1)}$ with $P_{BA}(t)$ from BA pressure recordings and t_1, t_2 denote the start and end time point of a cardiac cycle. Collectively, we examined the changes in these hemodynamic parameters and indices in zebrafish at 3, 4, 5 dpf that revealed functional changes in cardiac performance of the developing heart.

Statistical Treatment

Results from intraventricular pressure ($PSVP$, $EDVP$, and HR) were expressed as mean ± SD of the measurement with $n = 5$ for each of 3, 4, 5 dpf time point. Results from reconstructed ventricular volume and derived parameters (SV, EF, CO) were expressed as mean ± SD with $n = 3$ for each time point. Results incorporating measurements from the BA (TPR and $\overline{P_{BA}}$) were expressed as means ± SD with $n = 3$ for each of three time points. Differences in each of $PSVP$, $EDVP$, HR, SV, EF, CO, SW, $\overline{P_{BA}}$ and TPR among time points were tested for with a one-way ANOVA followed by Tukey's multiple comparison test with $p < 0.05$ chosen for statistical significance.

RESULTS

Representative time courses of intraventricular pressure measurements, reconstructed ventricular volume, blood flow rate, and regulating valve activities over two cardiac cycles are presented in Figs. 3, 4 and 5 for embryonic zebrafish at 3, 4, and 5 dpf, respectively. In Figs. 4 and 5, red vertical dash lines demarcate the four phases of the cardiac cycle: filling, isovolumic contraction, ejection, and isovolumic relaxation. No data is reported for valves at 3 dpf, since the remodeling of valve leaflets is yet to be complete at this point in development. In Fig. 3, ECG signals from 3 dpf zebrafish, adapted from Dhillon *et al.*,[4] was used to time scale our measurement data to the known corresponding physiological events in the heart. Key hemodynamic parameters extracted from these measurements are summarized with statistics in Table 1 and depicted in Figs. 6a–6d.

Intra-ventricular Pressure

From embryos at 3 dpf, the $PSVP$ were found to be at 7.52 ± 0.77 mmHg. At 4, 5 dpf, their $PSVP$ were found to increase to 10.64 ± 1.64, to 11.26 ± 1.31 mmHg respectively, accounting for 41% and 50% increases above that at 3 dpf. The changes in $EDVP$ appeared to undergo a relatively small decrease from 1.36 ± 0.52 to 1.28 ± 0.31 to 1.32 ± 0.19 mmHg, accounting for 6% and 3% decreases from that at 3 dpf. There were significant increases in $PSVP$ between 3 and 4 dpf groups ($p = 0.0063$) and between 3 and 5 dpf groups ($p = 0.0017$), however, the change in $EDVP$ was not significant.

From pressure recordings, we found the HR to be at 112.87 ± 8.58, 130.02 ± 5.04, and 139.16 ± 6.70 beats/min for 3, 4, and 5 dpf embryos, respectively. Statistical testing indicated a statistically significant difference from 3 to 4 dpf ($p = 0.005$), and from 3 to 5 dpf ($p = 0.001$). While there was no significant difference when comparing the HR of 4 to 5 dpf ($p = 0.134$). All data of intraventricular pressure measurement are included in Supplementary Materials Fig. S2.

Ventricular Volumes, Stroke Volume, Cardiac Output, and Ejection Fraction

The EDV were found to be 0.18 ± 0.02 nL from 3 dpf embryos. The EDV values were found to increase to 0.33 ± 0.02 and 0.40 ± 0.03 nL from embryos at 4 and 5 dpf, respectively. Their corresponding values in ESV were found to be 0.08 ± 0.01 nL from embryo at 3 dpf, which increased to 0.14 ± 0.01 and 0.18 ± 0.01 nL from embryos at 4 and 5 dpf, accounting for 73% and 134% increases, respectively.

From 3 dpf embryos the SV was 0.10 ± 0.01 nL. From 4 and 5 dpf groups their SV were found to increase to 0.19 ± 0.01 and 0.21 ± 0.02 nL, which account for 96% and 120% increases from that at 3 dpf. Using HR measurements, the CO was calculated at 10.5 ± 0.6 nL/min at 3 dpf, which increased to 25.3 ± 1.7 at 4 dpf and then to 29.1 ± 2.18 nL/min at 5 dpf. CO at the latter two time points account for 142% and 178% increases, respectively, compared to 3 dpf values. Calculated EF were found to bear no significant changes, being 55.3 ± 2.4%, 58.3 ± 0.9% and 53.6 ± 0.5% from embryos at 3, 4 and 5 dpf, respectively.

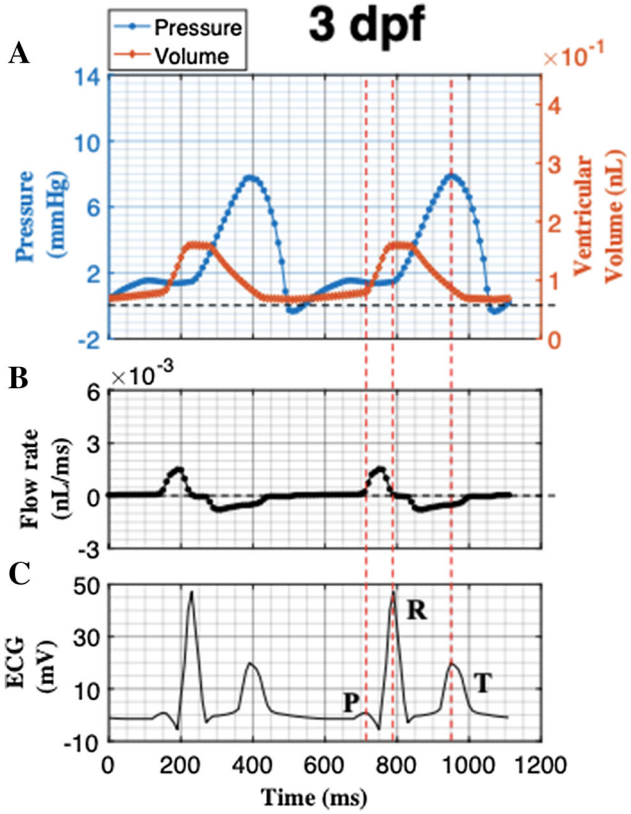

FIGURE 3. Representative time course of (a) Intra-ventricular pressure and ventricular volume, (b) Moment-to-moment blood flow rate calculated as the time derivative of the ventricular volume over two cycles from developing zebrafish heart at 3 dpf, (c) ECG signals from zebrafish at 3 dpf with P, R, T waves marked, adapted from Dhillon *et al.*[4] with time scaled to our measurements. Pressure and volume data are representative of measurements with $n = 5$ for pressure and $n = 3$ for volume, see Table 1 and Fig. 6 for statistical details.

Calculated Blood Flow Rates

During filling phase, from 3 dpf embryo we noted very little blood flow from atrium to ventricle until the onset of atrium contraction and reached a peak of 1.5×10^{-3} nL/ms. From 4 and 5 dpf embryos, the flow rates were also slow but reached a peak at 5.1 and 4.5×10^{-3} nL/ms, respectively, at atrial contraction. Hence there were increases in the peak values of inflow rate by 200–240 % from 3 to 4, 5 dpf. During ejection phase, we found a peak outflow of -0.8×10^{-3} nL/ms from 3 dpf embryos. From 4 and 5 dpf embryos, the peaks in outflow rates were found to be at -2.5 and -2.5×10^{-3} nL/ms, respectively, at ventricular contraction. That is, the peaks in outflow rates were found to increase by 213% from 3 to 4, 5 dpf. From the plots of blood flow rates, we noted that in both filling and ejection phases, it took longer time duration for the embryonic zebrafish at 3 dpf than that at 4 and 5 dpf, being ~ 280 ms and 180 ms from 3 dpf, as summarized in Table 2.

Pressure–Volume Loops

Representative pressure–volume loops constructed from synchronized intra-ventricular pressure measurements and reconstructed ventricular volume are presented in Fig. 7 for embryonic zebrafish at 3, 4 and 5 dpf, respectively. The *SW*, the mechanical work performed by the myocardium to pump the blood, was found to be 0.062 ± 0.008 nJ from embryo at 3 dpf, which increased to 0.158 ± 0.020 and 0.200 ± 0.023 nJ at 4 and 5 dpf, accounting for increases of 154% and 222%, respectively, from that at 3 dpf. It is noted that from 4 to 5 dpf, the increase in *SW* was 26%. The power generation of the developing embryonic heart was calculated to be 0.11 ± 0.01 nano-Watts at 3 dpf, became 0.35 ± 0.04 and 0.46 ± 0.06 nano-Watts at 4 and 5 dpf, respectively, accounting for a 218% and 315% increase over that at 3 dpf.

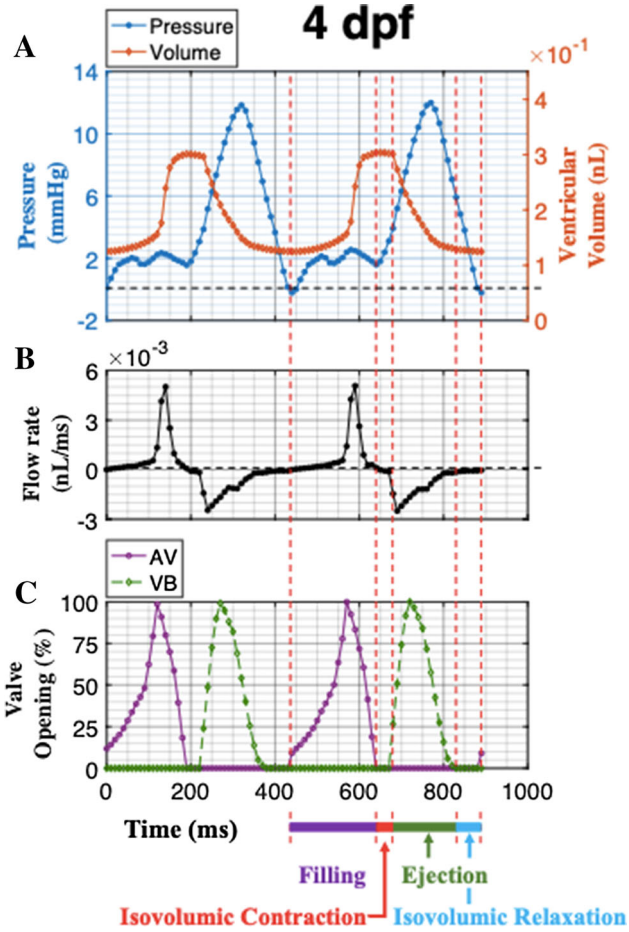

FIGURE 4. Representative time course of (a) Intraventricular pressure and ventricular volume, (b) Moment-to-moment blood flow rate calculated as the time derivative of the ventricular volume, and (c) Valve activities (Normalized) over two cycles from developing zebrafish heart at 4 dpf. Four phases in the cardiac cycle can be identified as marked. Pressure and volume data are representative of measurements with *n* = 5 for pressure and *n* = 3 for volume, see Table 1 and Fig. 6 for statistical details.

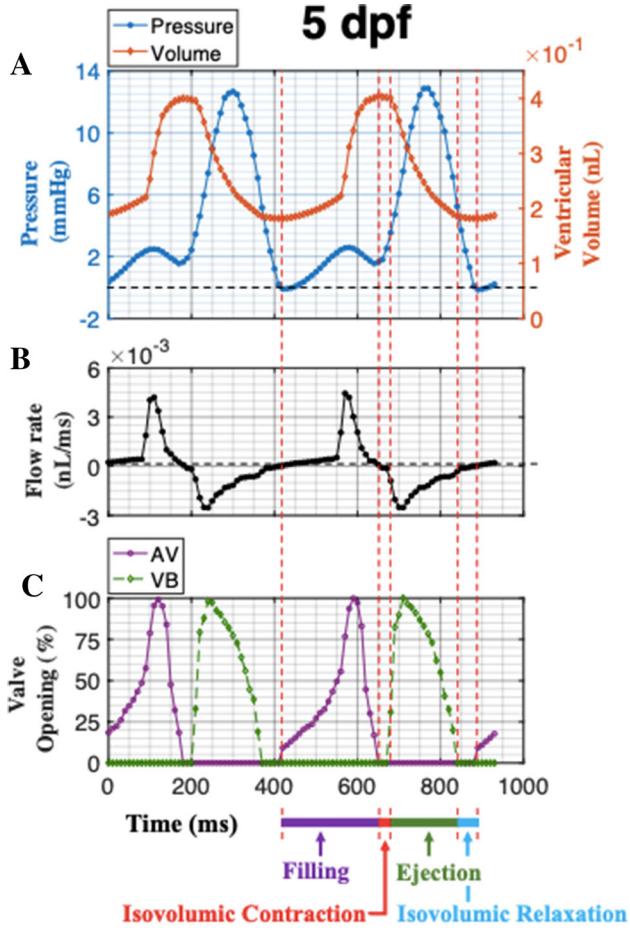

FIGURE 5. Representative time course of (a) Intraventricular pressure and ventricular volume, (b) Moment-to-moment blood flow rate calculated as the time derivative of the ventricular volume, and (c) Valve activities (Normalized) over two cycles from developing zebrafish heart at 5 dpf. Four phases in the cardiac cycle can be identified as marked. Pressure and volume data are representative of measurements with *n* = 5 for pressure and *n* = 3 for volume, see Table 1 and Fig. 6 for statistical details.

BA Pressure and TPR

To evaluate *TPR*, we calculated the mean of BA pressure $\overline{P_{BA}}$ from pressure-time recordings over a cardiac cycle in three fish per time point. $\overline{P_{BA}}$ was found to be 4.900 ± 0.339 mmHg at 3 dpf, which increased to 9.865 ± 0.646 and 9.944 ± 0.045 mmHg for the 4 and 5 dpf groups, respectively. These changes correspond to 101% and 103% increases compared to 3 dpf. Statistically significant differences were noted from 3 to 4 dpf ($p = 0.001$) and 3 to 5 dpf ($p = 0.001$), but not from 4 to 5 dpf ($p = 0.9$). Using the mean of $\overline{P_{BA}}$ values, a decreasing trend in *TPR* was established. At 3 dpf, *TPR* was found to be 0.504 ± 0.035 (mmHg. min/nL). This value then dropped to 0.423 ± 0.028 and 0.357 ± 0.002 (mmHg min/nL) in 4 and 5 dpf embryos, respectively, indicating a decrease of 16% and 29% respectively compared to 3 dpf. Statistically significant differences were noted from 3 to 4 dpf ($p = 0.021$), 3 to 5 ($p = 0.001$), and 4 to 5 dpf ($p = 0.043$). All data of BA pressure measurement are included in Supplementary Materials Fig. S3.

DISCUSSION

Significance

During development, the heart transforms from a linear peristaltic tube into a multi-chambered pulsatile pump.[31] Developmental changes in hemodynamic parameters have been reported in chick,[9,12,29,30] in mouse[11] and in zebrafish.[1,10,14,27] Few studies have systematically assessed the changes in cardiac performance of the developing zebrafish, and to our knowl-

TABLE 1. Hemodynamic parameters of developing Tg(*cmlc2:* mcherry*; fli1a:* gfp*)* zebrafish at 3, 4 and 5 dpf. (% in parenthesis indicates % changes from that of 3 dpf).

Parameters	Units	3 dpf	4 dpf	5 dpf
PSVP (Peak Systolic Ventricular Pressure) *n = 5 for each dpf group*	mmHg	7.52 ± 0.77	10.64 ± 1.64 (↑ 41%)	11.26 ± 1.31 (↑ 50%)
EDVP (End Diastolic Ventricular Pressure) *n = 5 for each dpf group*	mmHg	1.36 ± 0.52	1.28 ± 0.31 (↓ 6%)	1.32 ± 0.19 (↓ 3%)
EDV (End Diastolic Volume) *n = 3 for each dpf group*	nL	0.18 ± 0.02	0.33 ± 0.02 (↑ 86%)	0.40 ± 0.03 (↑ 126%)
ESV (End Systolic Volume) *n = 3 for each dpf group*	nL	0.08 ± 0.01	0.14 ± 0.01 (↑ 73%)	0.18 ± 0.01 (↑ 134%)
SV (Stroke Volume) *n = 3 for each dpf group*	nL	0.10 ± 0.01	0.19 ± 0.01 (↑ 96%)	0.21 ± 0.02 (↑ 120%)
HR (Heart Rate) *n = 5 for each dpf group*	beats/min	112.87 ± 8.58	130.02 ± 5.04 (↑ 15%)	139.16 ± 6.70 (↑ 23%)
CO (Cardiac Output) *n = 3 for each dpf group*	nL/min	10.5 ± 0.6	25.3 ± 1.7 (↑ 142%)	29.1 ± 2.18 (↑ 178%)
EF (Ejection Fraction) *n = 3 for each dpf group*	%	55.3 ± 2.4	58.3 ± 0.9 (↑ 5%)	53.6 ± 0.5 (↓ 3%)
SW (Stroke Work) *n = 3 for each dpf group*	nJ	0.062 ± 0.008	0.158 ± 0.020 (↑ 154%)	0.200 ± 0.023 (↑ 222%)
Power *n = 3 for each dpf group*	nano Watts	0.11 ± 0.01	0.35 ± 0.04 (↑ 218%)	0.46 ± 0.06 (↑ 315%)
$\overline{P_{BA}}$ (Mean BA pressure) *n = 3 for each dpf group*	mmHg	4.900 ± 0.339	9.865 ± 0.646 (↑101%)	9.944 ± 0.045 (↑ 103%)
TPR (Total Peripheral Resistance) *n = 3 for each dpf group*	mmHg min/nL	0.504 ± 0.035	0.423 ± 0.028 (↓16%)	0.357 ± 0.002 (↓29%)

Unit conversion: 1 mmHg nL = 0.133 nJ; 1 nL = 10^6 μm^3.

edge, no studies have integrated multiple physiological signal detection techniques to build a pressure–volume (PV) loop model of the developing zebrafish heart. In this work, we quantified and compared the mechanical performance of the developing zebrafish heart at 3, 4 and 5 dpf through an array of hemodynamic parameters. We constructed the resultant PV loops of the embryonic zebrafish heart by combining the direct intra-ventricular pressure measurements with reconstructed ventricular volumes, which enabled measurement of the changing mechanical performance of the developing zebrafish heart.

Cardiac disease model organisms often retain phenotypes with altered cardiac morphology and compromised cardiovascular physiology. Genetic manipulation may result in gene variants with a phenotype that cannot be obviously morphologically defined. An adverse physiological phenotype in a model organism could be just as insidious as in humans, where a physical examination may be required to diagnose some cardiovascular pathology. Thus, there is a need for rigorous quantification methods of physiological function in intact small animal models to relate physiological data to other vertebrate models and human health.

Improving Hemodynamic Performance of the Developing Heart

It has been reported that cardiac physiology exhibits rapid changes during early development, with a rapidly increasing intra-ventricular pressure and *CO* to meet the demands of the growing embryos.[5] Our results show that in zebrafish, *HR* increased by approximately 15% from 3 to 4 dpf, and by 23% from 3 to 5 dpf. On the other hand, *SV* nearly doubled between 3 and 4 dpf, with further increase up to 120% at 5 dpf. We determined a resultant 142% increase in *CO* from 3 to 4 dpf, which became 178% at 5 from 3 dpf. Indeed, the increase in *CO* at 4 and 5 dpf was due mainly to the increase in *SV*. This is not surprising, since 3-4 dpf zebrafish largely rely on diffusion for oxygenation. Over the next days, inhibitory cholinergic tone develops, slowing the resting heart rate, and pumping efficiency increases as the valves and cardiac tissues mature. Our calculated *SV* and *CO* are systematically lower than values previously reported for zebrafish[1] which is unsurprising given that these studies relied on an empirical formula derived from brightfield microscopy image capture.[23]

In both chick and mouse ventricles, *PSVP* increases faster than *EDVP* over early developmental stages.[9,11] Two studies[10,14] have reported intra-ventricular pressure measurement for zebrafish embryos, but to our knowledge there is no published data which use a calculated *SW* to assess the mechanical pump performance of the zebrafish ventricle. Our calculations showed that the *SW* for the zebrafish heart on 4 dpf was 2.5 times that of the *SW* in 3 dpf hearts. At 5 dpf, the *SW* increased to 3.2× that of 3 dpf. It is therefore interesting to note the power generation of the developing zebrafish heart as compared to the human heart. Here, 3–5 dpf zebrafish hearts were found to generate between 0.1 and 0.46 nano-Watts of power, whereas that of a typical human adult generates closer to 1.4 watts.[8]

Our analysis of the evolving mechanical function of the developing zebrafish heart indicates that significant improvement in cardiac performance occurs between 3 and 4 dpf. This is not surprising, since we see the valves becoming effective near 4 dpf. Comparatively smaller changes were detected between 4 and 5 dpf. The embryonic zebrafish heart generated higher pressure

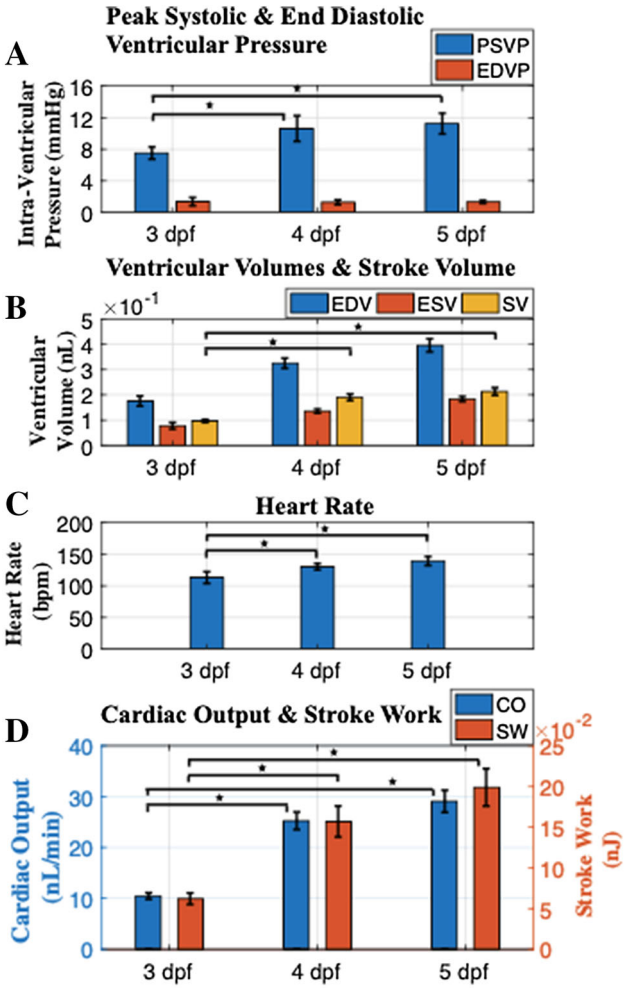

FIGURE 6. Comparison of (a) Intra-ventricular pressure (n = 5), (b) Ventricular volumes (n = 3), (c) Heart Rates (n = 5), and (d) Cardiac Output and Stroke Work (n = 3), among developing zebrafish heart at each of 3, 4, and 5 dpf. *PSVP*: Peak Systolic Ventricular Pressure; *EDVP*: End Diastolic Ventricular Pressure; *EDV*: End diastolic volume; *ESV*: End systolic volume; *SV*: Stroke volume; *CO*: Cardiac Output; *SW*: Stroke Work. In (a)–(d) statistically significant differences are denoted by *.

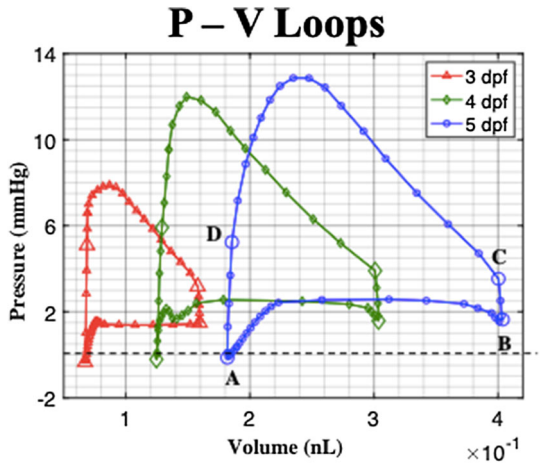

FIGURE 7. Representative pressure–volume (PV) loops of the developing zebrafish heart at 3, 4, and 5 dpf. Open markers (a), (b), (c), (d) designate time steps with valve activities where (a): AV valve open; (b): AV valve close; (c): VB valve open; (d): VB valve close. Four phases of a cardiac cycle: Segment AB—ventricular filling; Segment BC—isovolumic contraction; Segment CD—ventricular ejection; and Segment DA—isovolumic relaxation.

TABLE 2. Time duration of filling and ejection phases from embryonic zebrafish at 3, 4, 5 dpf.

	Filling			Ejection		
dpf	Start (ms)	End (ms)	Duration (ms)	Start (ms)	End (ms)	Duration (ms)
3	510	790	**280**	840	1020	**180**
4	440	640	200	680	830	150
5	420	650	230	680	840	160

At each dpf, the time duration of filling is calculated as the difference of the end and the start time points of the filling phase, whereas the time duration of ejection is calculated as the difference of the end and the start time points of the ejection phase.
Start and end time points refer to the results of Figs. 3b, 4b and 5b.

TABLE 3. Two steps ventricular filling and their respective contribution, both in the unit of nL and % of the total volume increase, from embryonic zebrafish at 3, 4, and 5 dpf.

	Filling							
	Step 1			Step 2			Ejection	
		Volume increase			Volume increase			
dpf	Δt (ms)	(nL)	%	Δt (ms)	(nL)	%	Δt (ms)	Volume decrease (nL)
3	210	0.015	16	70	0.077	84	180	0.091
4	130	0.032	18	70	0.147	82	150	0.175
5	140	0.041	18	90	0.181	82	160	0.22

Also listed are the corresponding time duration and ventricular volume decrease during the ejection phase.

throughout contributing to the increasing higher *CO* of the rapidly growing embryo. Collectively, our results suggest that the zebrafish heart is a well-developed functional organ near 5 dpf, in time for upcoming increased demand on the gills for respiration and osmoregulation.[24]

TPR values were found to decrease in embryonic zebrafish from 3 to 4 to 5 dpf groups, corresponding to a 16% decrease from 3 to 4 dpf, and 29% decrease from 3 to 5 dpf. Our results suggest the combined effects of a higher *PSVP, SV, CO* and *SW* lead to a progressively more powerful and efficient working heart to achieve the noted improvement in functional capacity. Through the growth, there are more cardiomyocytes and ventricular mass engaged in the pumping effort of the heart to deliver oxygen and nutrients to the growing body mass of the zebrafish. The decrease in TPR from 3–5 dpf is indicative of the increasing complexity of the perfusion pattern in the developing zebrafish, a general pattern seen in chick and anuran embryos, and likely a vertebrate paradigm for hemodynamic development.[7]

Examining the PV Loop: Negative Intra-ventricular Pressure

Our measurements showed intra-ventricular pressure dropped to negative values at the end of isovolumic relaxation (Fig. S2). We attributed this to the rapid isovolumic relaxation of the ventricular myocardium, along with a corresponding rapid ventricular pressure drop (high dp/dt). A slight negative intra-ventricular pressure can help to draw blood into the ventricle for 3 dpf embryos, when valve cushions are not yet fully functional valves. For embryos at 4, 5 dpf, the negative intra-ventricular pressure likely helps to open the AV valve. Blood influx immediately decelerates in the ventricle, converting its kinetic energy into potential energy, as intra-ventricular pressure increases. This transient event sets the stage for the filling phase.

A Twostep Filling Phase, ECG Signals and Time of Atrial Contraction

Ventricular filling consists of two steps. In step 1, driven by the atrium-ventricular pressure gradients, the blood influx is relatively slow. The onset of step 2 is evidenced by both the rapid increase in flow rate, attributed to both atrial contraction (occurring just after the P wave in the ECG (Fig. 3c)), and the rapid opening of the AV valve leaflets in embryonic zebrafish at 4, 5 dpf. We summarized the time duration for each of the two-step filling and the ejection phases in Table 3 with their respective contribution in volume and in percentage of the total volume increase through the filling phase. These data reveal that ventricular filling and ejection tasks take longer for embryonic zebrafish at 3 dpf compared to later stages, likely due to less developed cardiac tissue, valves and innervation.

Ventricular peak filling rate was almost 2 times the peak ejection rate. This relative increase was due in part to the relatively low ventricular pressure and hence low impedance throughout most of the filling phase but is primarily due to vigorous atrial contraction. Two-step filling has been previously reported for zebrafish embryos at 6.2 dpf[20] and adult zebrafish[34] with the majority of filling taking place during atrial systole.

Estimation of Ventricular Volume Using 2D Images with Axisymmetric Assumption

Other investigators have estimated ventricular volumes using 2D image sequences of the mid plane of the heart with an axisymmetric assumption.[1,23,27] To assess

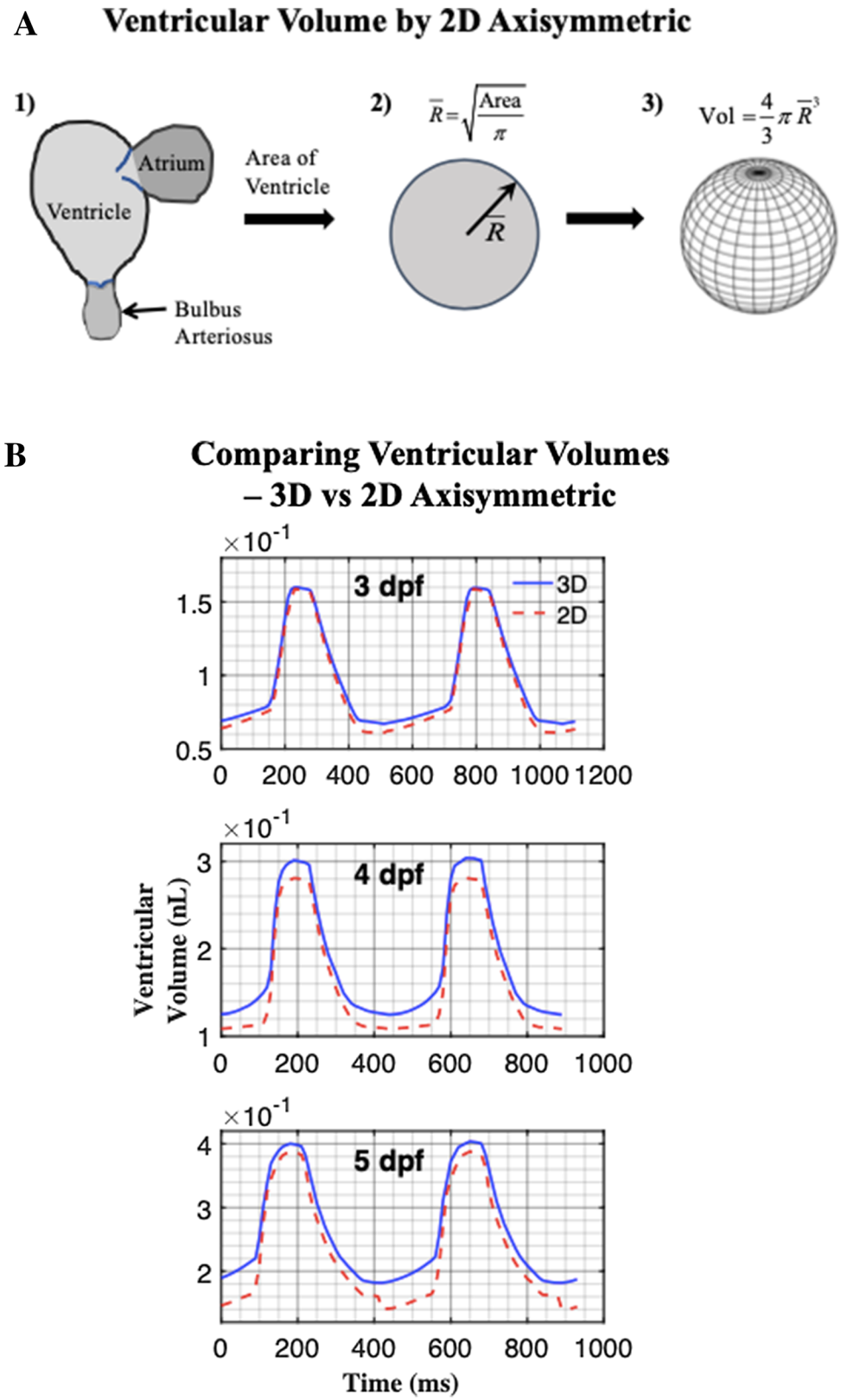

FIGURE 8. (a) Method of ventricular volume measurement using 2D images of the heart. (1) By manual segmentation, endocardial perimeter of the ventricle was identified, (2) Equivalent radius was calculated from the ventricular area, (3) Ventricular volume was estimated using axisymmetric sphere assumption. (b) Comparison between ventricular volume of developing zebrafish heart at 3, 4 and 5 dpf, estimated from 3D images and from 2D images using axisymmetric assumption.

the corresponding level of approximation in ventricular volume with the 2D approach, we manually segmented 2D image sequences of the mid-plane of embryonic zebrafish heart to delineate the endocardial boundary of the ventricle. From its enclosed area, we found the effective radius of the equivalent circle with the same surface area. At each time step, the ventricular volume was calculated from the corresponding equivalent circle based on axisymmetric spherical assumption (Fig. 8a). We found that the use of 2D images with axisymmetric assumption can lead to an underestimation artifact when calculating cardiac output. Indeed, for the 3 dpf, zebrafish, the 2D approach was associated with a 10% underestimation of the 3D calculated volume. Surprisingly, the 2D method underestimated up to 23% less volume for embryos at 4 and 5 dpf (Fig. 8b). Not surprisingly, this significant underestimation of ventricular volume occurred during the early part of ventricular filling, when the ventricle assumed a narrowed shape at the end of systole.

LIMITATIONS

Separate animals were used for pressure measurements and volume calculations. As such, PV loop data from cardiac cycles represent paired ventricular pressure and volume from separate embryos at each time point following the synchronization steps described in Methods. It was not possible to use the same animal for both pressure and volume measurement because direct measurement of ventricular pressure is destructive, rendering the organism unusable for additional experiments. Otherwise, early attempts to complete imaging prior to pressure recordings proved unfeasible due to the time required for acquiring micro-pressure measurements and the prolonged effects of anesthesia to capture both measurements from one fish (>2 h). Further, though the addition of PTU to suppress pigmentation is generally accepted as being unharmful, we do note that PTU blocks the conversion of thyroid hormone, the master regulator of vertebrate metamorphosis. Though PTU addition is fairly common in such studies and the developmental progression here appears to proceed normally, it is not possible that PTU causes a hidden, yet deleterious effect on the developmental program.[18,35] An additional limitation to this study is the use of transgenic organisms. Here, we assumed that the gene variants in our experimental organisms had no effect on the physiological phenotype. Ironically, this study was initiated to develop new techniques to detect fine scale physiological changes using direct pressure measures combined with advanced imaging modality (SPIM). As such, these limitations point out knowledge gaps in the acquisition of real time physiological data from small model organisms and the need to develop experimental tools to detect unseen, yet potentially insidious physiological effects. With the emergence of the zebrafish as a premier biomedical model, it is prudent to consider the need for higher throughput, non-destructive and high resolution measures of animal physiology.

CONCLUSIONS

We reported the development of hemodynamic parameters of the embryonic zebrafish ventricle at 3, 4 and 5 dpf. At each time point, dynamic measurements of ventricular pressure and volume allowed a 4D reconstruction of changing pressure and volume during the cardiac cycle. This enabled, for the first time, the creation of a pressure–volume loop of the ventricle of the developing zebrafish. Improving mechanical performance of the heart as a pump was described in terms of increasing degree of stroke work performed by the ventricular myocardium. Our results revealed significant increases in peak systolic pressure, stroke volume, cardiac output, stroke work. Further, a concomitant decrease in *TPR* from 3 to 5 dpf tracked the increasing mechanical performance, indicating the development of an increasingly complex vascular pattern. These changes reflect both the very early stages of heart development at 3 dpf prior to heart valve formation, then later stages of the developing embryo heart at 4 and 5 dpf. Together these data illustrate increasing pumping efficiency in the developing zebrafish heart, to meet environmental challenges and further highlight the utility of capturing reliable physiological data at early developmental time points. Such physiological measures are increasingly important for the future of phenomics efforts, which seek to match complex phenotypes with underlying variations in genotype.

SUPPLEMENTARY INFORMATION

The online version of this article (https://doi.org/10.1007/s10439-021-02731-0) contains supplementary material, which is available to authorized users.

ACKNOWLEDGMENTS

We acknowledge the supports from the AHA Grant #18CDA34110150 (to JL), NSF Grant #1936519 (to JL) and the University of Texas Arlington.

COMPETING INTERESTS

All authors declare no competing interests.

REFERENCES

[1]Bagatto, B., and W. Burggren. A three-dimensional functional assessment of heart and vessel development in the larva of the Zebrafish (*Danio rerio*). *Physiol. Biochem. Zool.* 79:194–201, 2005.

[2]Burggren, W. W., B. Dubansky, and N. M. Bautista. Cardiovascular development in embryonic and larval fishes. In: Fish Physiology, edited by A. K. Gamperl, T. E. Gillis, A. P. Farrell, and C. J. Brauner. San Diego: Academic Press, 2017, pp. 107–184.

[3]Burggren, W. W., J. F. Santin, and M. R. Antich. Cardiorespiratory development in bird embryos: new insights from a venerable animal model. *Revista Brasileira de Zootecnia* 45:709–728, 2016.

[4]Dhillon, S. S., E. Doro, I. Magyary, S. Egginton, A. Sik, and F. Muller. Optimisation of embryonic and larval ECG measurement in zebrafish for quantifying the effect of QT prolonging drugs. *PLoS ONE* 8:e60552, 2013.

[5]Goenezen, S., M. Y. Rennie, and S. Rugonyi. Biomechanics of early cardiac development. *Biomech. Model. Mechanobiol.* 11:1187–1204, 2012.

[6]Gurung, S., B. Dubansky, C. A. Virgen, G. F. Verbeck, and D. W. Murphy. Effects of crude oil vapors on the cardiovascular flow of embryonic Gulf killifish. *Sci. Total Environ.* 751:141627, 2021.

[7]Hou, P. C., and W. W. Burggren. Cardiac output and peripheral resistance during larval development in the anuran amphibian *Xenopus laevis*. *Am. J. Physiol.* 269:R1126–R1132, 1995.

[8]Houghton, D., T. W. Jones, S. Cassidy, M. Siervo, G. A. MacGowan, M. I. Trenell, and D. G. Jakovljevic. The effect of age on the relationship between cardiac and vascular function. *Mech. Ageing Dev.* 153:1–6, 2016.

[9]Hu, N., and E. B. Clark. Hemodynamics of the stage 12 to stage 29 chick embryo. *Circ. Res.* 65:1665–1670, 1989.

[10]Hu, N., D. Sedmera, H. J. Yost, and E. B. Clark. Structure and function of the developing zebrafish heart. *Anat. Rec.* 260:148–157, 2000.

[11]Ishiwata, T., M. Nakazawa, W. T. Pu, S. G. Tevosian, and S. Izumo. Developmental changes in ventricular diastolic function correlate with changes in ventricular myoarchitecture in normal mouse embryos. *Circ. Res.: J. Am. Heart Assoc.* 93:857–865, 2003.

[12]Keller, B. B., J. P. Tinney, and N. Hu. Embryonic ventricular diastolic and systolic pressure-volume relations. *Cardiol. Young* 4:19–27, 1994.

[13]Kirkman, E. Mechanical events and the pressure–volume relationships. *Anaesth. Intensive Care Med.* 19:314–317, 2018.

[14]Kopp, R., T. Schwerte, and B. Pelster. Cardiac performance in the zebrafish breakdance mutant. *J. Exp. Biol.* 208:2123–2134, 2005.

[15]Lee, J., P. Fei, R. R. Sevag Packard, H. Kang, H. Xu, K. I. Baek, N. Jen, J. Chen, H. Yen, C. C. Kuo, N. C. Chi, C. M. Ho, R. Li, and T. K. Hsiai. 4-Dimensional light-sheet microscopy to elucidate shear stress modulation of cardiac trabeculation. *J. Clin. Investig.* 126:3158, 2016.

[16]Lee, J., V. Vedula, K. I. Baek, J. Chen, J. J. Hsu, Y. Ding, C. C. Chang, H. Kang, A. Small, P. Fei, C. M. Chuong, R. Li, L. Demer, R. R. S. Packard, A. L. Marsden, and T. K. Hsiai. Spatial and temporal variations in hemodynamic forces initiate cardiac trabeculation. *JCI Insight* 3:e96672, 2018.

[17]Li, J., Y. Cao, Y. Wu, W. Chen, Y. Yuan, X. Ma, and G. Huang. The expression profile analysis of NKX2-5 knockout embryonic mice to explore the pathogenesis of congenital heart disease. *J. Cardiol.* 66:527–531, 2015.

[18]Li, Z. R., D. Ptak, L. Y. Zhang, E. K. Walls, W. X. Zhong, and Y. F. Leung. Phenylthiourea specifically reduces zebrafish eye size. *PLoS ONE* 7:14, 2012.

[19]Liebling, M., A. S. Forouhar, M. Gharib, S. E. Fraser, and M. E. Dickinson. Four-dimensional cardiac imaging in living embryos via postacquisition synchronization of nongated slice sequences. *J. Biomed. Opt.* 10:054001–0540010, 2005.

[20]Liebling, M., A. S. Forouhar, R. Wolleschensky, B. Zimmermann, R. Ankerhold, S. E. Fraser, M. Gharib, and M. E. Dickinson. Rapid three-dimensional imaging and analysis of the beating embryonic heart reveals functional changes during development. *Dev. Dyn.* 235:2940–2948, 2006.

[21]Messerschmidt, V., Z. Bailey, K. I. Baek, R. Bryant, R. Li, T. K. Hsiai, and J. Lee. Light-sheet fluorescence microscopy to capture 4-dimensional images of the effects of modulating shear stress on the developing zebrafish heart. *J. Vis. Exp.: JoVE* 138:e57763, 2018.

[22]Moriyama, Y., F. Ito, H. Takeda, T. Yano, M. Okabe, S. Kuraku, F. W. Keeley, and K. Koshiba-Takeuchi. Evolution of the fish heart by sub/neofunctionalization of an elastin gene. *Nat. Commun.* 7:10397, 2016.

[23]Perrichon, P., M. Grosell, and W. W. Burggren. Heart performance determination by visualization in larval fishes: influence of alternative models for heart shape and volume. *Front. Physiol.* 8:464, 2017.

[24]Rombough, P. The functional ontogeny of the teleost gill: Which comes first, gas or ion exchange? *Comp. Biochem. Physiol. A Mol. Integr. Physiol* 148:732–742, 2007.

[25]Salman, H. E., B. Ramazanli, M. M. Yavuz, and H. C. Yalcin. Biomechanical investigation of disturbed hemodynamics-induced tissue degeneration in abdominal aortic aneurysms using computational and experimental techniques. *Front. Bioeng. Biotechnol.* 7:111, 2019.

[26]Scherz, P. J., J. Huisken, P. Sahai-Hernandez, and D. Y. Stainier. High-speed imaging of developing heart valves reveals interplay of morphogenesis and function. *Development* 135:1179–1187, 2008.

[27]Shin, J. T., E. V. Pomerantsev, J. D. Mably, and C. A. MacRae. High-resolution cardiovascular function confirms functional orthology of myocardial contractility pathways in zebrafish. *Physiol. Genom.* 42:300–309, 2010.

[28]Steed, E., F. Boselli, and J. Vermot. Hemodynamics driven cardiac valve morphogenesis. *Biochim. Biophys. Acta* 1863:1760–1766, 2016.

[29]Stekelenburg-de Vos, S., P. Steendijk, N. T. C. Ursem, J. W. Wladimiroff, R. Delfos, and R. E. Poelmann. Systolic and diastolic ventricular function assessed by pressure-volume loops in the stage 21 venous clipped chick embryo. *Pediatric Res.* 57:16–21, 2005.

[30]Stekelenburg-de Vos, S., P. Steendijk, N. T. Ursem, J. W. Wladimiroff, and R. E. Poelmann. Systolic and diastolic ventricular function in the normal and extra-embryonic venous clipped chicken embryo of stage 24: a pressure-

volume loop assessment. *Ultrasound Obstet. Gynecol.* 30:325–331, 2007.
[31]Taber, L. A., and R. Perucchio. Modeling heart development. *J. Elast.* 61:165–197, 2000.
[32]Vermot, J., A. S. Forouhar, M. Liebling, D. Wu, D. Plummer, M. Gharib, and S. E. Fraser. Reversing blood flows act through klf2a to ensure normal valvulogenesis in the developing heart. *PLoS Biol.* 7:e1000246, 2009.
[33]Walley, K. R. Left ventricular function: time-varying elastance and left ventricular aortic coupling. *Crit. Care* 20:270, 2016.
[34]Wang, L. W., I. G. Huttner, C. F. Santiago, S. H. Kesteven, Z.-Y. Yu, M. P. Feneley, and D. Fatkin. Standardized echocardiographic assessment of cardiac function in normal adult zebrafish and heart disease models. *Dis. Models Mech.* 10:63–76, 2017.
[35]Wang, W. D., Y. Wang, H. J. Wen, D. R. Buhler, and C. H. Hu. Phenylthiourea as a weak activator of aryl hydrocarbon receptor inhibiting 2,3,7,8-tetrachlorodibenzo-p-dioxin-induced CYP1A1 transcription in zebrafish embryo. *Biochem. Pharmacol.* 68:63–71, 2004.
[36]Weber, M., and J. Huisken. In vivo imaging of cardiac development and function in zebrafish using light sheet microscopy. *Swiss Med. Wkly* 145:w14227, 2015.
[37]Westerfield, M. The zebrafish book : a guide for the laboratory use of zebrafish (*Brachydanio rerio*). Eugene, OR: M. Westerfield, 1993.
[38]Yalcin, H. C., A. Amindari, J. T. Butcher, A. Althani, and M. Yacoub. Heart function and hemodynamic analysis for zebrafish embryos. *Dev. Dyn.* 246:868–880, 2017.
[39]Zakaria, Z. Z., F. M. Benslimane, G. K. Nasrallah, S. Shurbaji, N. N. Younes, F. Mraiche, S. I. Da'as, and H. C. Yalcin. Using zebrafish for investigating the molecular mechanisms of drug-induced cardiotoxicity. *Biomed. Res. Int.* 2018. https://doi.org/10.1155/2018/1642684.